Medium effects in $(\pi,\pi'\gamma)$ angular correlations on $^{12}C(2^+)$

R. Olszewski,* R. Baran, A. Hofmann, S. Krell,† H. W. Ortner, J. Orzechowsky, G. Schmidtlein, and F. Vogler
Physikalisches Institut der Universität Erlangen-Nürnberg, D-8520 Erlangen, Federal Republic of Germany

W. List and G. R. Smith‡
Kernforschungszentrum, Institut für Kernphysik und Institut für Experimentelle Kernphysik der Universität Karlsruhe, D-7500 Karlsruhe, Federal Republic of Germany

D. Dehnhard
University of Minnesota, Minneapolis, Minnesota 55455

M. Thies
Natuurkundig Laboratorium der Vrije Universiteit, 1007 MC Amsterdam, The Netherlands
(Received 13 October 1987)

Pion-γ angular correlations have been measured both in and out of the reaction plane for the reaction $^{12}C(\pi,\pi')^{12}C^*(2^+, 4.44\ \text{MeV})$, $^{12}C^* \rightarrow {}^{12}C(\text{g.s.})+\gamma$. Data are presented at a pion momentum transfer of $q=0.47\ \text{fm}^{-1}$ for incident pion energies of 116, 140, 162, 180, and 226 MeV and at $q=0.85\ \text{fm}^{-1}$ for energies of 116, 162, and 226 MeV. A detailed description of the experimental setup together with the applied test procedures and of the data analysis is given. The data are compared to predictions of the Δ-hole model and its static limit.

I. INTRODUCTION

Because of the dominance of Δ excitation in pion-nucleon scattering at intermediate energies, pion-nucleus scattering provides an excellent tool with which to investigate to what extent the behavior of the Δ resonance excited in the nucleus is influenced by the nuclear medium. For the theoretical description of the resonance dominated pion-nucleus scattering the so-called Δ-hole model has been developed[1,2,3,4,5] and applied first to pion-nucleus elastic scattering. Lenz *et al.*[6] used this approach to describe pion-nucleus inelastic scattering retaining the phenomenological parameters from fits to the elastic scattering data.

In the Δ-hole formalism Δ-hole states are introduced explicitly and are allowed to propagate leading to a nonlocal transition operator. Binding and Pauli corrections are calculated microscopically, while more complex Δ-nucleus interactions like those arising from pion absorption in nonmesonic channels are treated phenomenologically through a Δ-nucleus spreading potential.

To get a reference point for the dynamical phenomena treated in the Δ-hole model, the static limit of this formalism can be considered, in which the Δ-nucleus dynamics is eliminated completely.[6] Thus medium corrections and Δ propagation are neglected in this limit.

In inelastic pion scattering reactions to discrete final states of a nucleus, the Δ-hole model often yields a description of the differential cross sections nearly equivalent to that from calculations in the static limit. For these reactions the consideration of the magnetic substate population of the excited state is of particular interest. On the one hand the transition amplitudes for the different magnetic substates are expected to be more sensitive to medium effects than the more inclusive differential cross section; on the other hand, symmetry considerations within the Δ-hole model show that different excitation mechanisms populate the individual substates differently. Therefore, observables sensitive to the magnetic-substate populations are particularly suited to test the validity of the Δ-hole model.

Pion-gamma angular correlation data are sensitive to the magnetic substate population of pion scattering to a discrete final state with subsequent gamma decay. A first $(\pi,\pi'\gamma)$ experiment in the Δ-resonance region has been performed at the Swiss Institute for Nuclear Research (SIN) at a pion energy of 162 MeV on the $(2^+, 4.4\ \text{MeV})$ state in ^{12}C.[7] In this experiment no energy resolution was available for the scattered pions, and the angular correlation data were taken only in the reaction plane at a single incident energy. Already from these rather modest data there were indications that the Δ-nucleus dynamics was important for the description of the pion-nucleus interaction.

In a recent letter[8] we reported on a new $(\pi,\pi'\gamma)$ angular correlation experiment with considerably improved accuracy and range. Data for the angular correlation function were presented for measurements at a momentum transfer $q=0.47\ \text{fm}^{-1}$ and for five incident energies between 116 and 226 MeV. The purpose of this paper is to give a detailed description of the experimental setup together with the applied test procedures and monitoring systems, data analysis and discussion of statistical and systematic errors. We furthermore present additional data for a momentum transfer of $q=0.85\ \text{fm}^{-1}$ taken at incident energies of 116, 162, and 226 MeV. From the angular correlation data the coefficients and phases of the

angular correlation function as derived in Sec. II have been extracted and the results are discussed in detail by comparing them to the predictions of the Δ-hole model and the static limit of Ref. 6.

II. ANGULAR CORRELATION FORMALISM

The formalism of particle-γ angular correlations of the general type $A(a,b)B(\gamma)C$ has been presented in Ref. 9. In this work we apply that formalism to a $A(\pi\pi')$ reaction leading to an excited state with definite spin and parity, which then decays with the emission of a single γ ray. We choose the quantization (z) axis to point in the direction of $\mathbf{k}_i \times \mathbf{k}_f$ and the x axis in the direction of $\mathbf{k}_i$, where $\mathbf{k}_i$ and $\mathbf{k}_f$ denote the momenta of the incident and scattered pion, respectively. The definition of the reference frame, as well as the convention of angles referring to it and used in the text are illustrated in Fig. 1.

The double differential cross section for scattering a pion in the direction $\mathbf{k}_f$, while a γ ray is emitted along $\mathbf{k}_\gamma$ and its polarization is not detected, can be written as

$$\frac{d^2\sigma}{d\Omega_\pi d\Omega_\gamma} = \frac{W(\phi_\pi;\theta_\gamma,\phi_\gamma)}{4\pi}\frac{d\sigma}{d\Omega_\pi} . \tag{1}$$

The normalization of the angular correlation function $W(\phi_\pi;\theta_\gamma,\phi_\gamma)$ is found by integrating over the solid angle $d\Omega_\gamma$

$$\int W(\phi_\pi;\theta_\gamma,\phi_\gamma)d\Omega_\gamma = 4\pi . \tag{2}$$

Using the statistical tensors ρ^T_{KQ} as defined in Ref. 9 the angular correlation function takes the form

$$W(\phi_\pi;\theta_\gamma,\phi_\gamma) = \sum_{\substack{K,Q \\ K \text{ even}}} \frac{\rho^T_{KQ}}{\rho^T_{00}} R_K(\gamma) \times \left[\frac{4\pi}{2K+1}\right]^{1/2} Y_{KQ}(\theta_\gamma,\phi_\gamma) . \tag{3}$$

The factors $R_K(\gamma)$ depend only on the parameters of the γ transition. In case of pure multipole radiation they consist only of vector coupling coefficients.[10] The statistical tensors ρ^T_{KQ} are related to the density matrix elements $\rho_{MM'}$ by

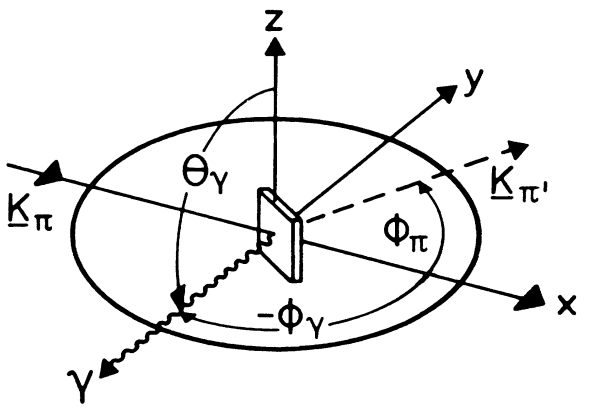

FIG. 1. The definition of the coordinate system.

$$\rho^T_{KQ} = \sum_{M,M'} (-1)^{J-M'}(JJM-M' \mid KQ)\rho_{MM'} \tag{4}$$

with the density matrix itself given by

$$\rho_{MM'} = T_{JM}T^*_{JM'} , \tag{5}$$

where T_{JM} is the transition amplitude for the considered state with angular momentum J and projection M.

With the proper normalization of the transition amplitude the differential cross section is given by the incoherent sum over the magnetic substates

$$\frac{d\sigma}{d\Omega_\pi} = \sum_M |T_{JM}|^2 . \tag{6}$$

In deriving the following relations we restrict ourselves to the investigated reaction $^{12}C(\pi,\pi')^{12}C(2^+)(\gamma)^{12}C$, i.e., a $0^+ \to 2^+ \to 0^+$ spin sequence. The particular choice of the coordinate system establishes reflection symmetry with respect to the reaction plane. This allows the application of Bohr's theorem[11] which in turn leads to the requirement

$$T_{JM} = (-1)^M T_{JM} \tag{7}$$

Therefore only substates with even M, i.e., $M=-2,0,+2$ can be populated

With this result the angular correlation function written in terms of the density matrix elements is given by

$$W(\phi_\pi;\theta_\gamma,\phi_\gamma) = \{\tfrac{5}{4}(\rho_{22}+\rho_{-2-2})+\tfrac{15}{2}(1-\rho_{22}-\rho_{-2-2})\cos^2\theta_\gamma+\tfrac{5}{4}(6-5\rho_{22}-5\rho_{-2-2})\cos^4\theta_\gamma - \tfrac{5}{2}\sqrt{6}\,|\rho_{20}+\rho_{0-2}|\cos^2\theta_\gamma\sin^2\theta_\gamma\cos[2(\phi_\gamma+\phi_0)] - \tfrac{5}{2}|\rho_{2-2}|\sin^4\theta_\gamma\cos\{4(\phi_\gamma+\phi_2)\}\Big/\frac{d\sigma}{d\Omega_\pi} \tag{8}$$

where the phases ϕ_0 and ϕ_2 are defined by

$$\rho_{20}+\rho_{0-2} = |\rho_{20}+\rho_{0-2}|e^{i2\phi_0} , \qquad \rho_{2-2} = |\rho_{2-2}|e^{i4\phi_2} . \tag{9}$$

For the case $\theta_\gamma = 90°$, the so-called "in-plane" geometry, the angular correlation function W takes the well-known form

$$W(\phi_\pi;\theta_\gamma=90°,\phi_\gamma) = A + C\sin^2[2(\phi_\gamma+\phi_2)] . \tag{10}$$

According to Eq. (3) the coefficients A and C are given by

$$A=[\tfrac{5}{4}(\rho_{22}+\rho_{2-2})-\tfrac{5}{2}|\rho_{2-2}|]\Big/\frac{d\sigma}{d\Omega_\pi}\ ,$$
$$C=5|\rho_{2-2}|\Big/\frac{d\sigma}{d\Omega_\pi}\ . \tag{11}$$

Since quadrupole radiation with $M=0$ does not emit in directions perpendicular to the axis of quantization all contributions containing the transition amplitude T_{20} vanish in the in-plane correlation function. A complete determination of the angular correlation function thus requires the detection of γ rays out of the scattering plane. In the present work γ detectors have been placed at an angle of 45° below the reaction plane. We will refer to this choice of angles as to the "out-of-plane" geometry. In this case, i.e., $\theta_\gamma=45°$, and 135°, another oscillatory term enters the angular correlation function

$$W(\phi_\pi;\theta_\gamma=90°\pm45°,\phi_\gamma)=A'+C'\sin^2\{2(\phi_\gamma+\phi_2)\}+D\sin^2\{\phi_\gamma+\phi_0\}\ . \tag{12}$$

The new coefficient D now depends on the transition amplitude T_{20}

$$D=(\tfrac{5}{4}\sqrt{6}\,|\rho_{20}+\rho_{0-2}|)\Big/\frac{d\sigma}{d\Omega_\pi}\ , \tag{13}$$

whereas the coefficients A' and C' are related to the coefficients A, C, and D by

$$A'=\tfrac{1}{8}(15-6A-4C-4D)\ ,$$
$$C'=C/4\ . \tag{14}$$

This representation of the angular correlation function has been chosen for the presentation of our results. The coefficients A, C, and D and the phases ϕ_0 and ϕ_2 have been determined in the experiment. This is equivalent to a determination of the modulus of the transition amplitudes T_{2-2}, T_{20}, and T_{22} and of two of their relative phases.

In the nonlocality expansion of Ref. 6 the pion couples to a number of nuclear densities of increasing complexity. Neglecting terms of second and higher order one obtains four nuclear structure terms, the transition density (scalar), the spin density (vector), the convention current (vector) and the spin flux tensor. These modes of excitation can be taken into account by defining "even" (T^+_{JM}) and "odd" (T^-_{JM}) pieces in the transition amplitude T_{JM}, where T^+_{JM} corresponds to scalar/tensor excitations and T^-_{JM} to vector excitations.

In the coordinate system of Fig. 1, $T^\pm_{JM}$ and $T^\pm_{J-M}$ differ only by a complex phase factor.

$$T^\pm_{J-M}=\pm(-1)^J e^{2iM\phi_q}T^\pm_{JM}\ . \tag{15}$$

Here ϕ_q denotes the angle between the transferred momentum **q** and the incident pion momentum **k**,

$$\phi_q=\tfrac{1}{2}(\phi_\pi-180°)\ . \tag{16}$$

In terms of these amplitudes the in-plane angular correlation function can be written as[12]

$$W(\phi_\pi;\theta_\gamma=90°,\phi_\gamma)=\frac{5}{d\sigma/d\Omega_\pi}|T^-_{22}\cos^2 2(\phi_\gamma-\phi_q)+iT^+_{22}\sin^2 2(\phi_\gamma-\phi_q)|^2\ . \tag{17}$$

Obviously the coefficients A, C, and D and the phases ϕ_0 and ϕ_2 determined in our experiment can also be expressed in terms of T^+_{20} and $T^\pm_{22}$. In contrast to the amplitudes T_{20} and $T_{2\pm2}$ of Eq. (5), these amplitudes are directly related to the even and odd excitation modes.

III. EXPERIMENTAL PROCEDURE

The experiments were performed at the $\pi M1$ channel of the Schweizerisches Institut für Nuklearforschung. The SUSI pion spectrometer facility was used to detect scattered pions while an array of six NaI crystals detected the coincident γ rays. Details of the beamline and the spectrometer are given in Refs. 13 and 14. A schematic view of the detector arrangement is given in Fig. 2.

The target used was graphite with an areal density of 1.61 g/cm^2. The achieved energy resolution in the excitation spectra was about 1.4 MeV FWHM. The measurements used a pion flux of typically 5×10^6 π^+/sec. The proton contamination was chiefly reduced by an electrostatic separator. The momentum of the incident pions was measured at the intermediate dispersive focal plane of the beamline with a hodoscope $S1$ consisting of 16 scintillators, each with a thickness of 1.2 mm. It covered a momentum acceptance of $\delta p/p_0=1.5\%$.

A plastic scintillator $S2$ of 1 mm thickness was mounted 10 cm upstream of the scattering target to count the incident particles. It also served to discriminate against remaining protons by setting an upper threshold $S2^p$ on its pulse height. A beam event was then defined by a coincidence $S2\cdot\overline{S2}^p\cdot Rf$, where Rf denotes the cyclotron frequency signal.

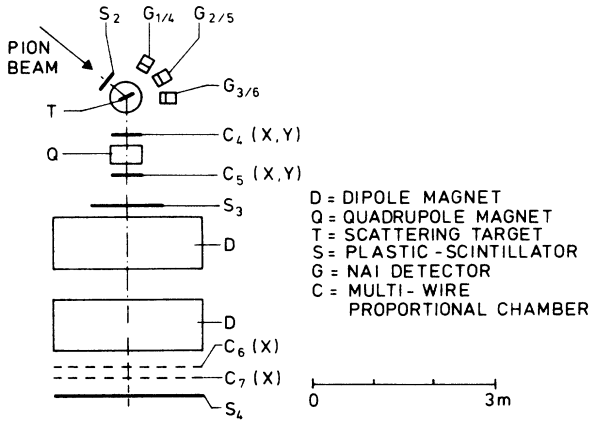

FIG. 2. Schematic diagram of the experimental setup.

Pions scattered from the carbon target were momentum analyzed by the SUSI spectrometer. The spectrometer is a vertically bending quadrupole-double dipole magnet system. The entrance quadrupole focuses in the horizontal plane. Two multiwire proportional chambers (MWPC) $C4$ and $C5$ are placed on either side of the quadrupole to define the trajectory of particles entering the system. The MWPC's $C6$ and $C7$ are mounted at the exit of the spectrometer crossing its focal plane. They allow for the determination of the trajectories of the exiting particles, and together with the information from $C4$ and $C5$ for the determination of the particle positions in the focal plane. The spectrometer field was set to keep the 4.4 MeV excitation region in the middle of the focal plane. Two scintillation counters $S3$ and $S4$ are mounted behind $C5$ and $C7$, respectively. The coincidence $S3 \cdot S4$ gives a trigger signal for the system and defines a spectrometer event. The solid angle of the spectrometer is approximately 16 msr with angular acceptance of $\pm 3°$ in the vertical and $\pm 5°$ in the horizontal direction.

The deexcitation γ rays were detected with six NaI counters of cylindrical shape. Four of them had a size of 12.7-cm diameter $\times$ 12.7-cm height, the remaining two of 7.6-cm diameter $\times$ 7.6-cm height. The six counters were arranged in three pairs of equal size with one detector placed in the reaction plane ($\theta_\gamma = 90°$) and the other one mounted at an angle of 45° below the scattering plane ($\theta_\gamma = 135°$). All three γ arms were mounted to the pivot axis of the pion spectrometer. Taking into account the periodicity of the angular correlation function the range of γ angles achieved was $35° \leq \phi_\gamma \leq 140°$.

Since instabilities of photomultipliers with large cathode surfaces are a well-known problem, extra steps were taken to monitor and record the gain of the NaI detectors. A 3 mm thin layer of uv lucite was inserted between the NaI crystal itself and the photomultiplier. It served as a lightguide for feeding the light from a green light-emitting diode (LED) into the phototube. The LED signals were used to monitor the gains of the detectors. This task was performed by an intelligent multichannel analyzer (MCA) based on a Z-80 microcomputer in connection with the high-level real time language PEARL.[15] The MCA accumulated LED spectra for each NaI detector once per minute. It determined the position of the LED peak and handed this result to the PDP 11/45 data acquisition computer. This information was used in the off-line analysis to correct the analog-to-digital converter (ADC) spectra of the NaI detectors for possible gain variations, which turned out to be of the order $\pm 5\%$ at most. A detailed description of the hardware and software of the MCA system together with its application in the present work is given in Ref. 16.

The position of the LED peak was also used for the energy calibration of the ADC spectra of the NaI counters. Before and after each measurement the LED line and NaI counters were energy calibrated with standard γ-ray sources such as ^{60}Co, ^{88}Y, and others. The light intensity of the LED was adjusted to give a peak position corresponding to 5.5 MeV. The LED peak was therefore well separated from the region covered by 4.4 MeV γ rays of the ^{12}C deexcitation.

Since the effective solid angles of the NaI detectors depend on their distances to the target spot, and on the size of the target spot, the beam profile and position were scanned at the beginning and end of each measurement using a 0.2 mm wide scintillator mounted on a step motor drive 5 cm downstream of the scattering target. This scintillator was removed from the beam path during the actual measurements. The information obtained from these scans was included in the determination of the product of efficiency and solid angle $\epsilon_\gamma d\Omega_\gamma$ as described in Sec. IV.

Two different types of events were defined in the hardware trigger. The first type were so-called correlation events for which a coincidence between a beam event, a spectrometer event and an event in one of the six γ-detectors was required:

$$(S2 \cdot \overline{S2}^{p} \cdot Rf) \cdot (S3 \cdot S4) \cdot (G1 \vee G2 \vee \cdots \vee G6) .$$

The second type of events defined were "free" scattering events, which only required a coincidence between a beam event and the spectrometer: $(S2 \cdot \overline{S2}^{p} \cdot Rf) \cdot (S3 \cdot S4)$. Because of the small solid angle covered by NaI detectors the rate of scattering events was about a factor of 10^3 higher than the rate of correlation events. Therefore only a well defined fraction of scattering events was recorded to tape.

It should be pointed out that the simultaneous measurement of the yield of coincident π-γ-events and of the yield of inelastic scattering is advantageous for the data analysis. In the determination of the values of the angular correlation function the uncertainties connected with the use of the pion spectrometer, i.e., solid angle, acceptance or pion decay, cancel out. This leads to a considerably improved accuracy of the data as compared to previous measurements.[7,17]

IV. DATA REDUCTION AND ANALYSIS

The values of the angular correlation function $W(\phi_\pi;\theta_\gamma,\phi_\gamma)$ can be evaluated in two independent ways. Both methods have been applied to the data to check the consistency of the results.

The first method is derived from Eq. (1) by writing the angular correlation function W as ratio of the double differential cross section $d^2\sigma/d\Omega_\pi d\Omega_\gamma$ and the differential cross section $d\sigma/d\Omega_\pi$. Inserting the experimentally determined quantities and recalling the fact that the yield for $(\pi,\pi'\gamma)$ events and the yield (π,π') events was measured simultaneously, the angular correlation function is simply given by

$$W = \frac{N_{(\pi,\pi'\gamma)}}{N_{(\pi,\pi')}} \times \frac{4\pi}{\epsilon_\gamma d\Omega_\gamma (1 - K_{\text{abs}})} \tag{18}$$

$N_{(\pi,\pi'\gamma}$ is the yield of coincident π and γ events stemming from the excitation of the (2^+, 4.4 MeV) state. $N_{(\pi,\pi')}$ is the yield of scattered pions leading to this excited state. $\epsilon_\gamma d\Omega_\gamma$ is the product of efficiency and solid angle of the γ detectors and K_{abs} accounts for self-absorption of the γ rays in the graphite target.

The yield $N_{(\pi,\pi'\gamma)}$ was obtained by integrating the peak of the (2^+, 4.4 MeV) state in the excitation energy spec-

tra of the correlation events. Two different types of background contribute to these spectra and were removed in the course of data reduction.

The first type comes from muons and electrons from the decay of scattered pions in the spectrometer and any other events which are caused by scattered pions not passing directly through the spectrometer (i.e., pions which scatter from the pole faces). This background is removed by a trajectory analysis of each event. The angle of the pions exiting the spectrometer is calculated from its coordinate in $C4$ and $C5$ and from its momentum and then compared to the angle measured by $C6$ and $C7$. This comparison allows one to reduce this background to about 3% of the events in the excitation spectra.[14]

The second type of background in the spectra of the correlation events was due to accidental coincidences caused by the significant background rate in the NaI detectors. This background could be reduced to a negligible amount by putting a tight cut on the time-of-flight (TOF) measured between the NaI detectors and the scintillator $S2$, and on the energy of the γ rays. An example of a TOF spectrum obtained with one of the 12.7-cm NaI detectors is shown in Fig. 3. The flat distribution of accidental coincidences is limited by the time window in the trigger electronics. The width of the peak of the prompt events is determined by the time resolution and was typically 3.5 nsec for the 12.7-cm detectors and 2.0 nsec for the 7.6-cm detectors. The mean μ and variance σ were determined by assuming a gaussian peak shape. Events with a TOF value outside of a window of $\pm 3\sigma$ around the mean μ were rejected from further analysis.

In Fig. 4 an ADC spectrum of 12.7-cm NaI detector is shown. The spectrum contains only those events which passed the TOF test. The photo and single escape peaks of the 4.4 MeV γ rays are clearly visible. These two peaks were used for the energy calibration. In cases where the statistics were not sufficient for the determination of the positions of the peaks with the required precision, the γ spectra were calibrated using the peak of the LED events (not shown in Fig. 4). Events which were accepted for the final analysis had to have a γ energy between 2.0 and 5.0 MeV. These two limits are marked in Fig. 4 by arrows.

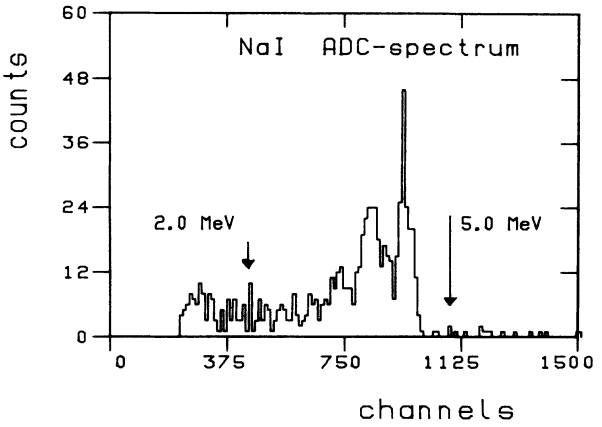

FIG. 4. Energy spectrum of the γ rays having passed the time-of-flight test. The events between the arrows are used in the analysis.

In Fig. 5 an example of an excitation energy spectrum of the correlation events is given. This spectrum contains only those events which passed the described tests. The counts in the ground state region are remaining accidental events. From the number of these events the contribution of accidentals to the $(2^+, 4.4\ \text{MeV})$ state can be estimated. The result was $\leq 1.0\%$ in all cases. The events in the excitation region above 15 MeV are of physical origin. Proton and neutron knockout lead to ^{11}B and ^{11}C as residual nuclei. Both nuclei have excited states around 4.4 MeV which decay by γ emission. Events of this type were the major cause of uncertainty in the first $(\pi,\pi'\gamma)$ experiment,[7] which did not use a spectrometer.

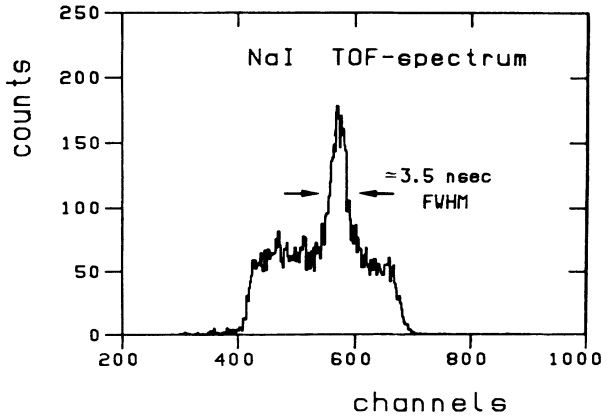

FIG. 3. Time-of-flight spectrum of the γ rays obtained with one of the 12.7×12.7-cm NaI detectors.

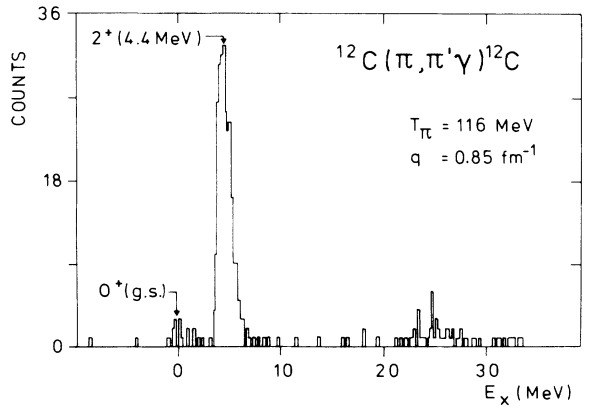

FIG. 5. Example of an energy spectrum of scattered pions in coincidence with 4.44 MeV γ rays detected in one of the NaI detectors.

The spectrum of scattered pions, obtained at $T_\pi = 116$ MeV and $\phi_\pi = 51°$ is shown in Fig. 6. As well as the 0^+ ground state and the 2^+ state at 4.4 MeV, the 3^- state at 9.6 MeV is pronounced at this momentum transfer. A least squares fit to the data was used to determine the peak integrals, i.e, $N_{(\pi,\pi')}$. The line shape of the peaks was derived from the peak of the (2^+, 4.4 MeV) state in the coincident spectra. The only free parameters in the fits of the spectra of the scattered pions were then the amplitudes of the peaks, an overall position and the coefficients of a quadratic background term.

The product of efficiency and solid angle $\epsilon_\gamma d\Omega_\gamma$ of the NaI detectors was measured in a separate $^{12}C(\alpha,\alpha'\gamma)$ experiment performed at the Erlangen tandem accelerator. The method used and the results obtained are presented in Ref. 18. The achieved accuracy for the values of $\epsilon_\gamma d\Omega_\gamma$ is $\pm 5\%$. The measured values of $\epsilon_\gamma d\Omega_\gamma$ had to be scaled for the detector distances in the present work, which deviated from the calibration distances by 10% at most. The uncertainty in the size of the beam spot and in the energy calibration of the γ-energy spectra led to an additional uncertainty in $\epsilon_\gamma d\Omega_\gamma$, which was thereby increased to $\pm 6\%$.

The factor K_{abs} finally corrects for absorption of the 4.4 MeV γ rays in the graphite target. It has been estimated[19] to vary from 1 to 3% depending on the angles of the NaI counters and of the target.

For the measurements at $q = 0.47$ fm^{-1} this method of evaluating the angular correlation function gave results with a rather poor accuracy. This was due to the fact that at the small momentum transfers the determination of the yield $N_{(\pi,\pi')}$ of the (2^+, 4.4 MeV) state was hampered by the dominance of the elastic scattering peak in the spectra. The lineshape of the peaks has a long tail towards higher excitation energies, which is caused by the small fraction of background events passing the muon test. The tail of the ground-state peak extends into the region of the (2^+, 4.4 MeV) state and at the forward scattering angles its contribution limits the accuracy in determining the peak integral of the (2^+, 4.4 MeV) state to 25%.

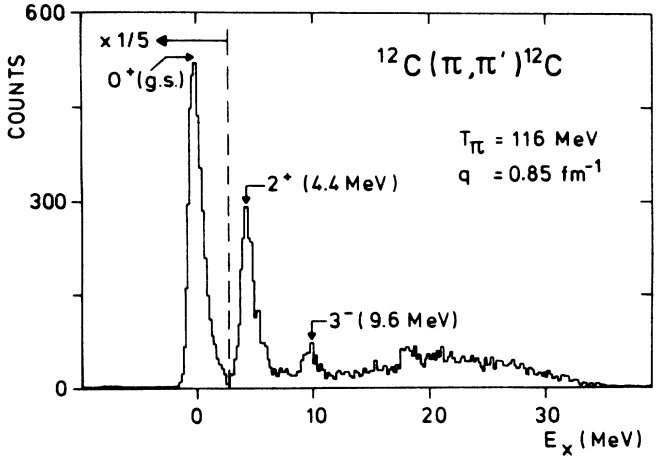

FIG. 6. Energy spectrum of the scattered pions obtained at $T_\pi = 116$ MeV and $\phi_\pi = 51°$ without coincidence requirement.

We therefore also applied a different method of analysis to the data by normalizing the individual runs to the elastic scattering yield N_{el} rather than to the yield $N_{(\pi,\pi')}$ of the (2^+, 4.4 MeV) state. By doing so an overall normalization factor F_{norm} is introduced, which is the ratio of the elastic cross section to the cross section of the (2^+, 4.4 MeV) state:

$$W = F_{norm} \times \frac{N_{(\pi,\pi'\gamma)}}{N_{el}} \times \frac{4\pi}{\epsilon_\gamma d\Omega_\gamma (1 - K_{abs})} . \tag{19}$$

The factor F_{norm} can be determined by using the normalization properties of the angular correlation function W as given in Eq. (2). In practice this is done by fitting the known analytical form [Eq. (8)] of the angular correlation function together with the overall normalization factor F_{norm}, to the data. The fits were performed with the code MINUIT (Ref. 20) using a least-squares method. The values of F_{norm} obtained from these fits agree with the ratio of previously measured cross sections[21] within the accuracy of our data.

This method led to an improved accuracy in determining the angular correlation values for the measurements at $q = 0.47$ fm^{-1}. For $q = 0.85$ fm^{-1} both methods resulted in similar uncertainties. Very good agreement between the values of the angular correlation function evaluated with the two different methods was found for all three energies at which data were taken for this momentum transfer.[19] For reasons of consistency all results presented in this paper have been obtained with the second method.

As a further result of the fit of the angular correlation function to the data, the coefficients A, C, and D, and the phases ϕ_0 and ϕ_2 were obtained. An error analysis as described in Ref. 22 was performed for the free parameters of the fit, the coefficients, the phases, and the normalization factor F_{norm}, thus, the stated uncertainties correspond to a 68% confidence level including correlations between the fit parameters.

It was necessary to include the finite solid angle of the NaI detectors and the pion spectrometer in fitting the angular correlation data. For the spectrometer only the opening angle in the vertical direction is of importance. Since the coefficients A, C, and D, and the phases ϕ_0 and ϕ_2 are functions of the pion scattering angle ϕ_π, the spectrometer acceptance in horizontal direction merely defines the angular bin over which these quantities were averaged. The acceptance was restricted in the offline analysis to $\pm 5°$, and found to be flat in this range. The effect of the finite solid angles on the results for the angular correlation coefficients and phases was studied by varying them separately. From this an additional error for the coefficients and phases could be estimated, which takes into account the uncertainty in the opening angles. This error was then added in quadrature to the error obtained from the code MINUIT.

V. THE RESULTS

In Figs. 7 and 8 the values of the angular correlation function are plotted versus the γ-emission angle ϕ_γ. Figure 7 shows the results for the momentum transfer $q=0.47$ fm^{-1}, which have been published previously,[8] and Fig. 8 for the momentum transfer $q=0.85$ fm^{-1}. The solid line is the result of the fit used to determine the normalization factor and the coefficients and phases of the angular correlation function. The good agreement between the data and the fits demonstrates the reliability of the measurements. The dashed curve is the prediction of the Δ-hole model. The dashed-dotted curve has been calculated in the static limit.

Instead of discussing the present values of the angular correlation function in detail, we present the extracted values for the coefficients A, C, and D, and the phases ϕ_0 and ϕ_2. These give a clearer and more detailed view of the underlying physics, and enable a more detailed and systematic comparison with the theoretical predictions.

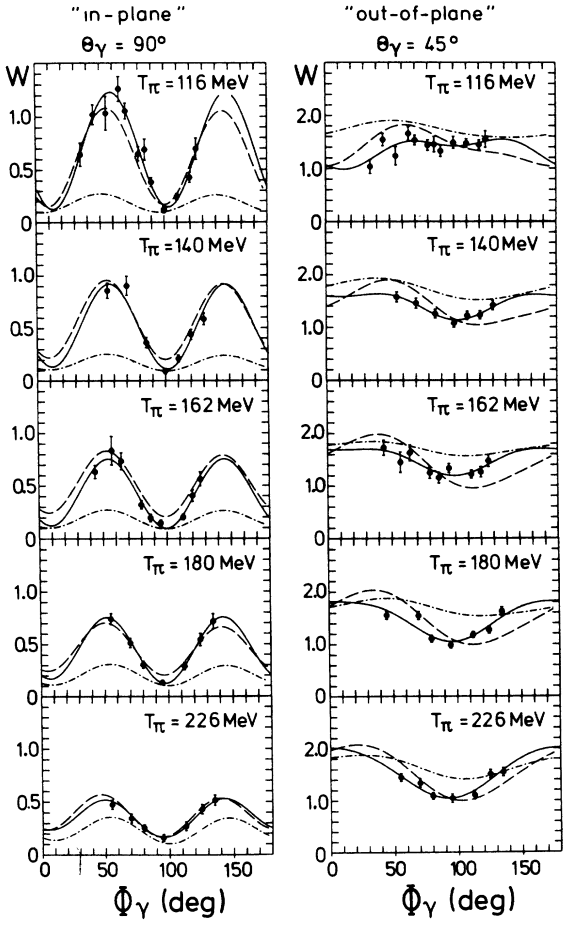

FIG. 7. In-plane and out-of-plane angular correlation function at a momentum transfer of $q=0.47$ fm^{-1} for different incident kinetic energies. The solid curves are best fits according to Eq. (8). The dashed and dashed-dotted curves represent predictions of the Δ-hole model and the static limit, respectively.

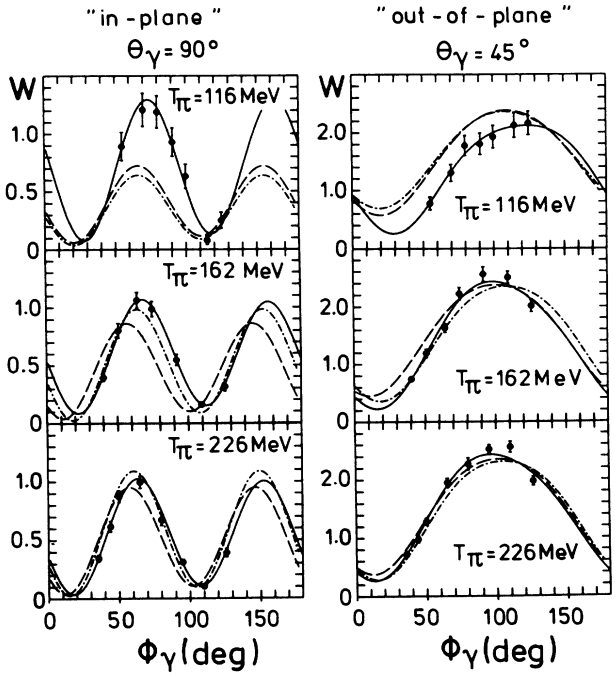

FIG. 8. Same as Fig. 7 at a momentum transfer $q=0.85$ fm^{-1}.

In Fig. 9(a) the values for the phase ϕ_2 are shown as function of the c.m. scattering angle ϕ_π of the pion. The solid line shows the relation between the phase ϕ_2 and the scattering angle ϕ_π as obtained in the adiabatic limit.[23] In this approximation the excitation of the nucleus is neglected and the differences between the initial and final kinetic energies of the particles involved are disregarded. The phase ϕ_2 is then given by $\phi_2=(\pi-\phi_\pi)/2$. The data are consistent with this simple relation. It seems therefore that the phase ϕ_2 depends merely on the kinematics of the reaction,[23] and thus a discussion of the behavior of the phase ϕ_2 as function of the bombarding energy is irrelevant.

It is, however, worth mentioning that the same relation between ϕ_2 and ϕ_π as in the adibatic limit is suggested by the Δ-hole model if we assume that the odd transition amplitude is zero or negligible compared to the even part [cf. Eq. (17)]. It should also be pointed out that because the phase ϕ_2 follows the adiabatic limit very closely, the odd amplitude $|T_{22}^-|$ is proportional to the coefficient A, whereas the even amplitude $|T_{22}^+|$ is proportional to the sum $(A+C)$.

The values for the phase ϕ_0 are presented in Fig. 9(b). Given that the even coupling dominates the transition, i.e., $|T_{22}^+| \gg |T_{22}^-|$, the Δ-hole model gives a relation between ϕ_0 and ϕ_π similar to the one for ϕ_2. It can easily be derived that $\phi_0=(\pi-\phi_\pi)/2$. If the real part of $T_{22}^+/T_{20}^{+*}e^{2i\phi_q}$ changes its sign the phase ϕ_0 changes by 90°. This leads to a second branch for ϕ_0 given by $\phi_0=\pi-\phi_\pi/2$. Both branches are shown as solid lines in

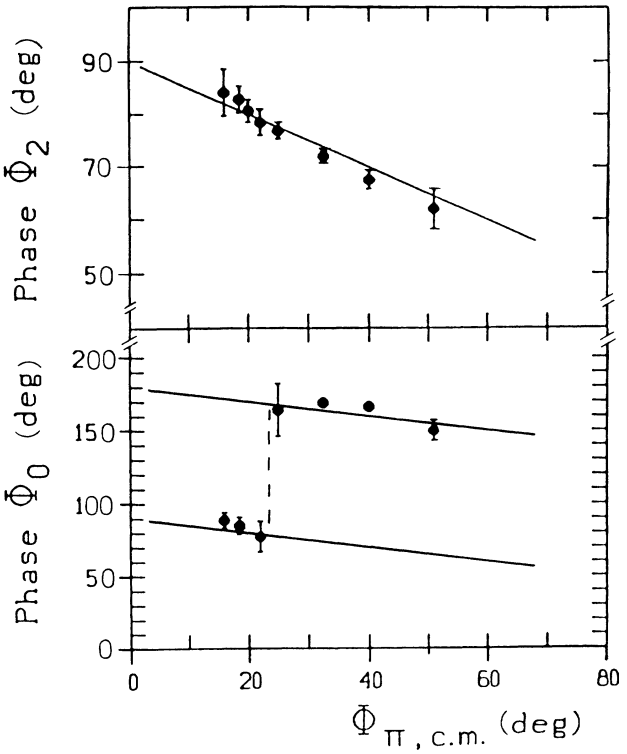

FIG. 9. The results for the phases ϕ_0 and ϕ_2. The solid lines correspond to the simple relations $\phi_2=(180°-\phi_\pi)/2$, $\phi_0=(180°-\phi_\pi)/2$, and $\phi_0=180°-\phi_\pi/2$.

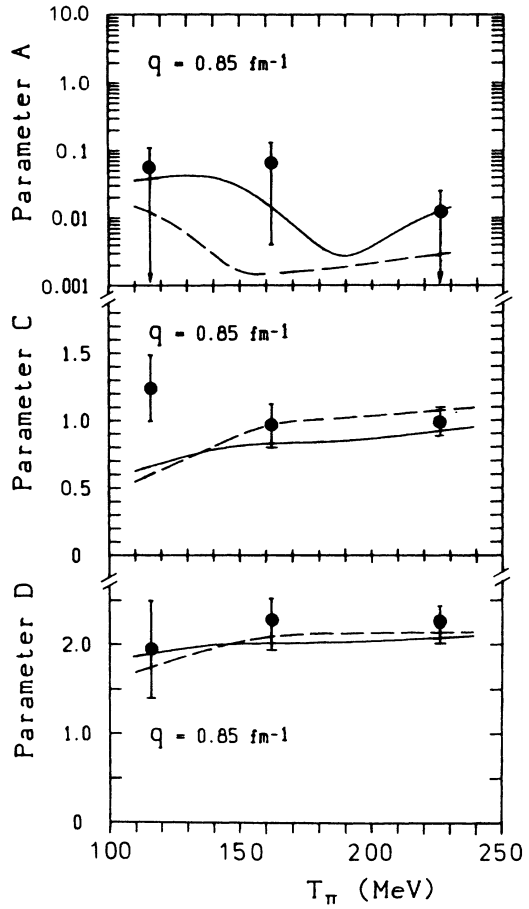

FIG. 10. The results for the coefficients A, C, and D of the angular correlation function for the momentum transfer $q=0.85$ fm^{-1}. The solid and dashed curves represent the predictions of the Δ-hole model and static limit, respectively.

Fig. 9(b). Again, the data follow these relations very closely and a transition between the two branches is actually observed (indicated by the dashed vertical line). The behavior of the phase ϕ_0 therefore also points to a small odd part in the transition, that means to small values for the parameter A.

For simplicity we have not shown the predictions of the Δ-hole model and the static model for the phases ϕ_0 and ϕ_2 in Fig. 9. Both models give very similar results for the phases which agree qualitatively with the data. In particular both models produce the transition between the two branches of the phase ϕ_0 at about the right scattering angle.

For the measurements with momentum transfer $q=0.85$ fm^{-1} the results for the coefficients A, C, and D of the angular correlation function are presented in Fig. 10 as function of the bombarding energy T_π. Also included in Fig. 10 are the predictions of the Δ-hole model (solid curve) and of the static model (dashed curve).

Both models give very similar predictions for all three coefficients (note the logarithmic scale for the coefficient A). At this particular momentum transfer the angular correlation function seems to be insensitive to the details of the reaction mechanism and therefore tests the DWIA formalism itself. The good overall agreement between the data and the theoretical predictions proves that the DWIA formalism is in general capable of describing angular correlation observables.

The coefficient A has small values over the whole measured energy range. This becomes more obvious if one notes that A can only take values between 0 and 1.25. The small values found are in agreement with the behavior of the phases ϕ_0 and ϕ_2. The large relative errors of the coefficient A are mainly caused by its strong sensitivity to the uncertainties in the finite solid angles of the detector equipment. The Δ-hole model gives consistently higher values for this coefficient than the static limit and is in slightly better agreement with the data. However, due to the large errors no firm conclusion can be drawn from this coefficient.

The coefficient D does not show a big variation with energy and is quantitatively described by the predictions of both models. The coefficient C also shows only little dependence on the bombarding energy. Its behavior is, however, in disagreement with the model predictions. The models predict decreasing values for C for lower bombarding energies. The experimental point for $T_\pi=116$ MeV clearly departs from the theoretical predictions and suggests a rising trend of the coefficient C at low incident energies. It is therefore interesting to note

that a detailed study of elastic and inelastic differential cross sections at $T_\pi = 100$ MeV found out, that neither the Δ-hole model nor the static limit can describe the angular distribution for the elastic and inelastic channels simultaneously.[24] An overall description of the cross sections of the measured states could be obtained by introducing an additional repulsive s-wave potential. The physical origin of such a potential is, however, unclear.

Figure 11 presents the results for the coefficients A, C, and D of the angular correlation function for the measurements with momentum transfer $q = 0.47$ fm^{-1}. The data (solid circles) are again shown as function of the kinetic energy T_π of the incident pion. The curves have the same meaning as in Fig. 10.

The coefficient A again has small values and, for the same reason as for $q = 0.85$ fm^{-1}, rather large relative errors. The predictions of the Δ-hole model are on the average a factor of 10 higher than the values in the static limit. For $q = 0.85$ fm^{-1} the difference is somewhat smaller, but also there the Δ-hole model produces higher values. At this point we should recall that due to the behavior of the phase ϕ_2 the coefficient A is directly proportional to the odd transition amplitude $|T_{22}^{-}|$. In the static limit this amplitude is given by the coupling to the magnetization density. In the Δ-hole model higher terms also contribute, in particular a convection current term. The predictions of the two models shown in Figs. 10 and 11 are the results of calculations where the transverse form factor has been parametrized as pure convection current. In the static limit the finite value of the coefficient A therefore results from the distortions of the pion waves only. In Ref. 25 it has, however, been shown that a satisfactory description of the transverse form factor over the total range of the momentum transfer covered with data[26] can only be obtained by using a coherent sum of magnetization density and convection current. Such a parametrization would imply increased values for the coefficient A in the static limit. In the Δ-hole model the magnetization density would add coherently to the convection current, either increasing or decreasing the values for A. With these shortcomings of the calculations in mind no further conclusions about the agreement between data and theory for the parameter A should be drawn.

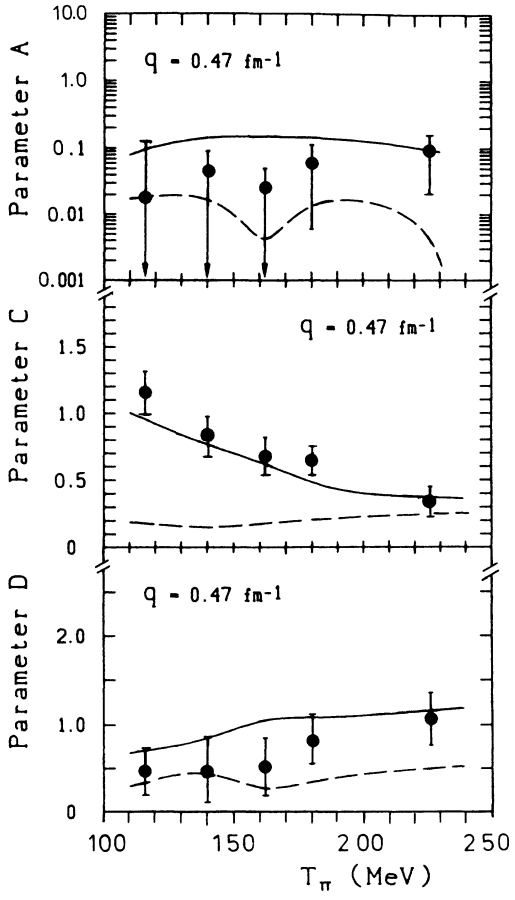

FIG. 11. The results of the coefficients A, C, and D of the angular correlation function for the momentum transfer $q = 0.47$ fm^{-1}. The meaning of the curves is the same as in Fig. 10.

The data for the coefficient D rise slowly with increasing bombarding energy. This general behavior is quite well reproduced by both models, although the Δ-hole model gives values which are a factor 3 to 4 higher than the values in the static limit. The big errors of the data, however, do not allow one to discriminate between the two models. The size of the errors is mainly due to the limitations in the accessible range of the azimuthal emission angle ϕ_γ of the γ rays. Because of the geometrical constraints in the present experimental arrangement data could only be taken in a region of $35° \leq \phi_\gamma \leq 140°$. This range covers a full period of the term $C \sin^2[2(\phi_\gamma + \phi_2)]$, but only half a period of the term $D \sin^2(\phi_\gamma + \phi_0)$. In comparison to the coefficient C the accuracy of the coefficient D is therefore rather poor.

The coefficient C has a very distinct energy behavior in the measured energy range. It decreases steadily from $C = 1.15$ at $T_m = 116$ MeV to $C = 0.34$ at $T_\pi = 226$ MeV. This behavior is also seen in the Δ-hole model calculations, which are in quantitative agreement with the data. The static limit, however, yields almost constant values of about 0.2 for the coefficient C at this momentum transfer and therefore cannot reproduce either the shape or the size of the data.

The Δ-hole model and its static limit yield very similar results for the differential cross section at a momentum tranfer of $q = 0.85$ fm^{-1}, which corresponds to the first diffractive maximum. At the lower momentum transfer of $q = 0.47$ fm^{-1}, however, there are significant differences between the two calculations, which result from the explicit treatment of the intermediate Δ resonance[6] in the Δ-hole model. These differences become smaller with increasing incident energies reflecting the fact that the static limit represents a "high-energy" approximation. For the coefficient C, which in contrast to the cross section contains the transition amplitudes $|T_{22}|$ and $|T_{2-2}|$ as a product [cf. Eqs. (11) and (5)], the differences between the predictions of the two models are considerably intensitied, and differ quite drastically with decreasing incident energy at $q = 0.47$ fm^{-1}.

Because of the behavior of the phase ϕ_2, which follows the adiabatic limit closely and because of the small values measured for the coefficient A, the coefficient C is approximately proportional to the even transition amplitude $|T_{22}^{+}|$. This amplitude depends strongly on the coupling of the pion to the transition density, which is given by the longitudinal form factor. This is the dominant excitation mode of the (2^+, 4.4 MeV) state. The nuclear wave functions used are reproducing the longitudinal form factor equally well in the relevant region of momentum transfer. Thus the differences in the predictions of the two models for the coefficient C cannot be explained with uncertainties in describing the nuclear structure of ^{12}C. The agreement between the data and the predictions of the Δ-hole model clearly demonstrate the importance of an elaborate microscopic treatment of the Δ propagation in pion nucleus scattering in the energy reigon of the Δ(3.3) resonance.

VI. CONCLUDING REMARKS

Our data show that at a pion energy corresponding to the maximum of the Δ-resonance, Δ-nucleus dynamics, as included in the Δ-hole model, is necessary to describe the pion-nucleon interaction in the nuclear medium. This follows mainly from the behavior of the amplitude C of the angular correlation function, which appears to be very sensitive to the reaction mechanism. At higher energies the predictions of the Δ-hole model and the static limit, which ignores the propagation of the intermediate Δ resonance, become similar, and both are in good agreement with our data. At lower energies there is a distinct disagreement in the correlation coefficient C between the experiment and both model predictions at a momentum transfer of 0.85 fm^{-1}, which corresponds to the first maximum of the cross section. Keeping in mind that important parameters used in the present model calculations are obtained from fits to the elastic scattering data, it remains to be seen, whether this disagreement can be removed by introducing a repulsive s-wave potential. Such a procedure improves the simultaneous description of elastic and inelastic cross sections in Ref. 24. On the other hand, it should be mentioned that in a recent study[27] of the Δ-nucleon interaction in pion-nucleus inelastic scattering, a phenomenological s-wave Δ-N interaction was used, which is consistent with the spreading potential determined in elastic scattering. In this study no appropriate parametrization for the Δ-N interaction could be found, which would yield a good description of both elastic and inelastic scattering. Furthermore, the effect of a refined treatment of the nonresonant amplitudes at energies away from the Δ resonance is unclear.

In order to get further insight into medium effects in the pion-nucleon interaction, especially at lower energies, we plan to extend our studies by measuring the dependence of the correlation function on the pion scattering angle. In particular, the structure of the angular distribution of the coefficient C should give additional information on the importance and details of the Δ-nucleus dynamics.

ACKNOWLEDGMENTS

One of us (D.D.) is greatly indebted to the kind hospitality extended to him at SIN, where part of the work was completed. This work has been supported by the German Bundesministerium für Forschung und Technologie.

*Present address: University of British Columbia, Vancouver, British Columbia, Canada V6T 2A3.

†Present address: Physikalisches Institut der Universität Tübingen, D-7000 Tübingen, Federal Republic of Germany.

‡Present address: TRIUMF, 4004 Wesbrook Mall, Vancouver, British Columbia, Canada V6T 2A6.

[1]L. S. Kisslinger and W. L. Wang, Ann. Phys. (N.Y.) **99**, 374 (1976).

[2]M. Hirata, F. Lenz, and K. Yazaki, Ann. Phys. (N.Y.) **108**, 116 (1977).

[3]K. Klingenbeck, M. Dillig, and M. G. Huber, Phys. Rev. Lett. **41**, 387 (1978).

[4]E. Oset and W. Weise, Nucl. Phys. **A329**, 365 (1979).

[5]M. Hirata, J. H. Koch, F. Lenz, and E. J. Moniz, Ann. Phys. (N.Y.) **120**, 205 (1979); Y. Horikawa, M. Thies, and F. Lenz, Nucl. Phys. **A345**, 386 (1980).

[6]F. Lenz, M. Thies, and Y. Horikawa, Ann. Phys. (N.Y.) **140**, 266 (1982).

[7]F. Vogler, R. Olszewski, M. Meyer, E. L. Mathie, G. R. Smith, E. Boschitz, S. Chakravarti, D. Dehnhard, and M. Thies, Phys. Lett. B **134**, 161 (1984).

[8]R. Olszewski, R. Baran, A. Hofmann, S. Krell, H. W. Ortner, J. Orzechowsky, G. Schmidtlein, F. Vogler, G. R. Smith, W. List, D. Dehnhard, and M. Thies, Phys. Rev. Lett. **57**, 2143 (1986).

[9]F. Rybicki, T. Tamura, and G. R. Satchler, Nucl. Phys. **A146**, 659 (1970).

[10]H. J. Rose and D. M. Brink, Rev. Mod. Phys. **39**, 306 (1969).

[11]A. Bohr, Nucl. Phys. **10**, 486 (1959).

[12]M. Thies, Nucl. Phys. **A412**, 326 (1984).

[13]J. P. Albanese, J. Arvieux, E. T. Boschitz, R. Corfu, J. P. Egger, P. Gretillat, C. H. Q. Ingram, C. Lunke, E. Pedroni, C. Perrin, J. Piffaretti, L. Pflug, E. Schwartz, C. Wiedner, and J. Zichy, Nucl. Instrum. Methods **158**, 363 (1979); J. Zichy, ETH Zürich, Dissertation No. 6612, 1979 (unpublished).

[14]C. H. Q. Ingram, P. A. M. Gram, J. Jansen, R. E. Mischke, J. Zichy, J. Bolger, E. T. Boschitz, G. Pröbstle, and J. Arvieux, Phys. Rev. C **27**, 1578 (1983).

[15]Deutsches Institut für Normung, Programmiersprache PEARL, Teil 1, DIN 66253 (Beuth, Berlin, 1981); R. Besold, R. Baran, A. Hofmann, P. Holleczek, and R. Mueller, Nucl. Instrum. Methods A **250**, 534 (1986).

[16]R. Baran, R. Besold, A. Hofmann, R. Olszewski, and H. W. Ortner, Nucl. Instrum. Methods A **258**, 91 (1987).

[17]R. J. Sobie, T. E. Drake, J. Gaydos, R. R. Johnson, R. Tacik, D. R. Gill, B. K. Jennings, and N. de Takacy, Phys. Lett. B **143**, 338 (1984).

[18]S. Krell, A. Hofmann, R. Olszewski, H. W. Ortner, and F. Vogler, Nucl. Instrum. Methods A **255**, 531 (1987).

[19]R. Olszewski, Ph.D. thesis, University of Erlangen, 1986 (un-

published).
[20]F. James and M. Roos, Comput. Phys. Commun. **10**, 343 (1975).
[21]W. B. Cottingame, K. G. Boyer, W. J. Braithwaite, S. J. Greene, C. J. Harvery, R. J. Joseph, D. B. Holtkamp, C. F. Moore, J. J. Kraushaar, R. J. Peterson, R. A. Ristinen, J. R. Shephard, G. R. Smith, R. L. Boudrie, N. S. P. King, C. L. Morris, J. Piffaretti, and H. A. Thiessen, Phys. Rev. C **36**, 230 (1987).
[22]F. James, Comput. Phys. Commun. **20**, 29 (1980).
[23]J. S. Blair and L. Wilets, Phys. Rev. **121**, 1493 (1961).
[24]L. E. Antonuk, D. Bovet, E. Bovet, J.-P. Egger, J.-F. Germond, F. Goetz, P. Gretillat, C. Lunke, E. Schwartz, K. Masutani, and T. Takaki, Nucl. Phys. **A420**, 435 (1984).
[25]D. Cha, Phys. Rev. C **21**, 1672 (1980).
[26]J. B. Flanz, R. S. Hicks, R. A. Lindgren, G. A. Peterson, A. Hotta, B. Parker, and R. C. York, Phys. Rev. Lett. **41**, 1642 (1978).
[27]T. Takaki, Ann. Phys. (N.Y.) **166**, 1 (1986).